Enhanced Peritoneal Ovarian Tumor Dissemination by Tissue Transglutaminase

Minati Satpathy,[1] Liyun Cao,[1] Roxana Pincheira,[8] Robert Emerson,[2] Robert Bigsby,[3,6] Harikrishna Nakshatri,[4,5,6,7] and Daniela Matei[1,3,5,6,7]

Departments of [1]Medicine, [2]Pathology and Laboratory Medicine, [3]Obstetrics and Gynecology, [4]Surgery, and [5]Biochemistry and Molecular Biology; [6]Indiana University Cancer Center; and [7]Walther Oncology Center, Indiana University School of Medicine, Indianapolis, Indiana and [8]Department of Surgery, University of California at San Francisco, San Francisco, California

Abstract

Tissue transglutaminase (TG2) is involved in Ca^{2+}-dependent aggregation and polymerization of proteins. We previously reported that TG2 *mRNA* is up-regulated in epithelial ovarian cancer (EOC) cells compared with normal ovarian epithelium. Here, we show overexpression of the TG2 protein in ovarian cancer cells and tumors and its secretion in ascites fluid and define its role in EOC. By stable knockdown and overexpression, we show that TG2 enhances EOC cell adhesion to fibronectin and directional cell migration. This phenotype is preserved *in vivo*, where the pattern of tumor dissemination in the peritoneal space is dependent on TG2 expression levels. TG2 knockdown diminishes dissemination of tumors on the peritoneal surface and mesentery in an i.p. ovarian xenograft model. This phenotype is associated with deficient β_1 integrin-fibronectin interaction, leading to weaker anchorage of cancer cells to the peritoneal matrix. Highly expressed in ovarian tumors, TG2 facilitates i.p. tumor dissemination by enhancing cell adhesion to the extracellular matrix and modulating β_1 integrin subunit expression. [Cancer Res 2007;67(15):7194–202]

Introduction

Epithelial ovarian cancer (EOC) arises from the epithelial layer covering the surface of the ovaries, and i.p. metastasis is commonly observed at diagnosis. Ovarian tumor spread in the i.p. space leads to the characteristic symptoms and complications of the disease, ascites, and small bowel obstruction. Several features set apart ovarian cancer spread from the metastatic model of other epithelial tumors. First, EOC cells are in direct contact with the overlying peritoneal fluid and this allows exfoliated cells to disseminate freely in the i.p. space. Second, ovarian cancer cells derived from the mullerian epithelium have dual epithelial and mesenchymal characteristics and can convert to either phenotype in response to factors in the microenvironment (1, 2). Adopting a mesenchymal phenotype favors dislodgement from the primary tumor, as cells are more motile and not bound by tight cellular junctions. Thus, EOC cells can spread passively to distant sites by exfoliating from the primary tumor, floating in the peritoneal fluid, and nesting along the i.p. space, where they adhere and grow as metastatic implants. This type of spread, which is uniquely characteristic to EOC, is accompanied by specific changes at the interface between tumor and the peritoneal "oncomatrix" that allow cancer cells to move, attach, and grow.

Such changes include increased expression of integrins (3–6) and of the hyaluran receptor CD44 (7) that promote adhesion of EOC cells to the peritoneum and overexpression of the chemokine receptor CXCR4 and secretion of its ligand CXCL12 that regulate cell motility in the i.p. milieu (8). Cancer and mesothelial cells secrete lysophosphatidic acid (9) and other proteins [fibronectin, periostin, osteopontin, and laminin (10–13)], which stabilize the extracellular matrix (ECM) and promote establishment of metastases. These interactions with the mesothelium and the peritoneal stroma activate "outside-in" signaling (14), which stimulates cancer cell proliferation and survival. In this context, neovascularization is facilitated and peritoneal metastases form and grow.

Tissue transglutaminase (TG2) is a ubiquitously expressed enzyme involved in protein cross-linking via acyl transfer between glutamine and lysine residues. TG2 promotes Ca^{2+}-dependent post-translational protein modification effected by the insertion of isopeptide bonds and incorporation of polyamines into peptide chains. We previously reported that TG2 *mRNA* expression is up-regulated in transformed ovarian epithelial cells and tumors compared with normal ovarian surface epithelial cells (15). Other reports link TG2 to epithelial cancers, particularly breast (16), pancreatic (17), and non–small cell lung cancer (18). In breast cancer cells, membrane-bound TG2 has kinase activity and phosphorylates the insulin-like growth factor-binding protein-3 (19) and the enzyme is overexpressed in drug- and radiation-resistant breast cancer cells (20, 21). The goal of this study was to analyze the role of TG2 as a mediator of ovarian tumor dissemination in the peritoneal space.

We show here that TG2 is expressed in a cancer-specific manner in human ovarian tumors and is secreted in ascites fluid. We show that TG2 facilitates ovarian cancer cell adhesion to fibronectin and directional cell migration and promotes i.p. tumor seeding. TG2 exerts its effects by interacting with β_1 integrin, modulating its expression and function. These data suggest a novel role for TG2 as a regulator of i.p. metastasis.

Materials and Methods

Immunohistochemistry. Twenty-seven paraffin-embedded epithelial ovarian tumor specimens from the Cooperative Human Tissue Collection and 6 normal ovarian specimens from six patients undergoing oophorectomy for benign disorders from the Indiana University Tissue Bank Collection were immunostained using a TG2 monoclonal antibody (CUB 7402, NeoMarkers) at a dilution of 1:200 after antigen retrieval using sodium citrate. Secondary labeling was based on the avidin/biotin system (LSAB2 kit, DAKO). Slides were stained with 3,3′-diaminobenzidine and counterstained with hematoxylin. Negative controls were run in parallel, with omission of the primary antibody. Staining was graded from 0 (no staining)

Note: Supplementary data for this article are available at Cancer Research Online (http://cancerres.aacrjournals.org/).

Requests for reprints: Daniela Matei, Division of Hematology-Oncology, Indiana University School of Medicine, 535 Barnhill Drive, RT 473, Indianapolis, IN 46202. Phone: 317-278-8844; Fax: 317-278-0074; E-mail: dmatei@iupui.edu.

doi:10.1158/0008-5472.CAN-07-0307

to 3+ (strong staining) by a board-certified pathologist. Immunoreactivity was recorded only if noted in more than 15% to 20% of tumor cells. The Indiana University Institutional Review Board approved the use of human tissue specimens (protocol 0412-54).

Ascites fluid. Thirty samples of ascites fluid cytologically positive from patients with ovarian cancer and 8 samples of ascites fluid from patients with noncancerous conditions (inflammatory pleural or ascitic fluid) were included in this analysis (University of California at Los Angeles and Indiana University Cancer Center Tissue Bank, protocol collection approved by the Institutional Review Board, protocol 0409-02). After collection, samples were centrifuged to remove cellular debris, aliquoted, and stored at −80°C until use.

Cell lines. Human SKOV3 and OV90 ovarian cancer cell lines were obtained from the American Type Culture Collection and cultured in growth medium containing 1:1 MCDB 105 (Sigma) and M199 (Cellgro) supplemented with 10% heat-inactivated fetal bovine serum (FBS; Cellgro) and 1% antibiotics (100 units/mL penicillin and 100 μg/mL streptomycin). All cells were grown at 37°C in a humidified 5% CO_2 atmosphere.

Transfection. To overexpress TG2, OV90 cells in the logarithmic phase of growth were transfected with wild-type TG2 cloned into the pcDNA3.1 vector using Fugene (Roche Applied Science). To knock down TG2, an antisense construct cloned into pcDNA3.1 vector was transfected in SKOV3 cells. As a control, cells were transfected with the pcDNA3.1 vector carrying the G418 resistance gene. Transfection efficiency in these conditions is typically 5% to 10% in OV90 cells and 30% to 40% in SKOV3 cells as determined by estimation of green fluorescent protein expression. Stable transfected clones were established by selection with G418 (Sigma) at concentrations of 600 μg/mL for SKOV3 cells and 150 μg/mL for OV90 cells. Plasmids were generous gift from Professor Janusz Tucholski (University of Alabama, Birmingham, AL). Overexpression and knockdown of TG2 in selected clones were shown by Western blot analysis.

Conditioned medium. Serum-free conditioned medium was collected from SKOV3 cells stably transfected with vector (pcDNA3.1) or the TG2 antisense construct (AS-TG2) and centrifuged at 3,000 rpm for 5 min to sediment cellular debris. Equal volumes of conditioned medium (30 μL) were used for immunoblotting.

Western blot analysis. Cells were lysed in radioimmunoprecipitation assay buffer containing protease inhibitors leupeptin (1 μg/mL), aprotinin (1 μg/mL), phenylmethylsulfonyl fluoride (PMSF; 400 μmol/L), and sodium orthovanadate (Na_3VO_4; 1 mmol/L). Cell lysates were sonicated briefly and subjected to centrifugation at 14,000 rpm for 15 min at 4°C to sediment particulate material. Equal amounts of protein (50 μg) were separated by SDS-PAGE and electroblotted onto polyvinylidene difluoride membranes (Millipore). After blocking, membranes were probed with primary antibody overnight at 4°C with gentle rocking. Antibodies used are β_1 integrin antibody (MAB2251, 1:1,000 dilution; Chemicon), TG2 (CUB 7402, 1:1,000 dilution), glyceraldehyde-3-phosphate dehydrogenase (GAPDH; 1:5,000 dilution; Biodesign International), and epidermal growth factor receptor (EGFR; 1:1,000 dilution; Cell Signaling). After incubation with specific horseradish peroxidase–conjugated secondary antibody, antigen-antibody complexes were visualized using the enhanced chemiluminescence detection system (Amersham Biosciences). Images were captured by a luminescent image analyzer with a CCD camera (LAS 3000, Fuji Film).

Separation of membrane and cytosolic proteins. SKOV3 cells were collected in a hypotonic lysis buffer containing 10 mmol/L KCl, 1.5 mmol/L $MgCl_2$, 10 mmol/L Tris-HCl (pH 7.4), and 2 mmol/L PMSF. The cell lysate was centrifuged at 4,000 × *g* for 15 min to remove cell debris and nuclei. The supernatant was then centrifuged at 100,000 × *g* for 60 min to separate the membrane fraction. The final crude membrane pellet was resuspended in a buffer containing 0.25 mol/L sucrose, 10 mmol/L Tris-HCl (pH 7.4), 150 mmol/L NaCl, and 2 mmol/L PMSF.

Coimmunoprecipitation. To detect the interaction between TG2 and β_1 integrin, SKOV3 cells were plated on fibronectin-coated (5 μg/mL) dishes, allowed to adhere for 2 h, and then lysed in a buffer containing 20 mmol/L Tris (pH 7.4), 150 mmol/L NaCl, 1 mmol/L β-glycerolphosphate, 1 mmol/L EDTA, 1 mmol/L EGTA, 1 mmol/L Na_3VO_4, 2.5 mmol/L sodium pyrophosphate, 1% Triton X-100, 10% glycerol, 1 μg/mL leupeptin, 1 μg/mL aprotinin, 400 μmol/L PMSF, and 1 mmol/L DTT. After 30 min of incubation on ice, cells were scraped from the plates, sonicated, and centrifuged at 14,000 rpm for 15 min to pellet cellular debris. Protein (500 μg) from the supernatant was incubated overnight at 4°C with β_1 integrin monoclonal antibody or mouse IgG (Santa Cruz Biotechnology). Immune complexes were recovered by adding 60 μL of a slurry of protein G plus/protein A agarose (Calbiochem) and shaking for 2 h at 4°C. After washing with a buffer containing 0.2% Triton X-100, the immune complexes were eluted with 2× sample buffer and boiled for 10 min at 100°C.

Reverse transcription-PCR. RNA was extracted from SKOV3 cells stably transfected with AS-TG2 or empty vector using RNA STAT-60 Reagent (Tel-Test, Inc.). RNA (2.5 μg) was used for first-strand cDNA synthesis using the SuperScript II System (Invitrogen). The following primers were used: β_1 integrin, ATCTGCGAGTGTGGTGTCTG (forward) and ACAACATGAACCATGACCTC (reverse); GAPDH, GATTCCACCCATGGCAAATTCC (forward) and CACGTTGGCAGTGGGGAC (reverse; Integrated DNA Technologies). The reverse transcriptase product (1 μL) and primers were heated at 94°C for 90 s followed by 28 rounds of amplification for GAPDH and 34 cycles for β_1 integrin (30-s denaturing at 94°C, 30-s annealing at 60°C, and 30-s extension at 72°C) followed by a final extension of 10 min at 72°C. The reverse transcription-PCR (RT-PCR) product was visualized under UV light after fractionation on a 1.5% agarose gel.

Immunofluorescence. SKOV3 cells were plated on fibronectin-coated chamber slides (BD Biosciences) and allowed to adhere. After fixation in 4% paraformaldehyde, cells were permeabilized using Triton X-100 (0.2% in PBS; 15 min) and blocked for 1 h with 3% goat serum in PBS. Then, cells were incubated for 2 h with primary antibody diluted in blocking buffer at room temperature [TG2 polyclonal antibody RB-060 (1:100 dilution; NeoMarkers) and β_1 integrin monoclonal antibody (MAB2251, 1:100 dilution)] followed by a 30-min incubation with AlexaFluor^{488} anti-mouse secondary antibody (1:1,000; Molecular Probes) or Cy5-conjugated anti-rabbit antibody (1:500; Zymed). Staining to visualize the cytoskeleton was done with rhodamine-phalloidin (Molecular Probes). Isotype-specific IgG served as a negative control. Nuclei were visualized by 4′,6-diamidino-2-phenylindole (DAPI) staining (Vectashield, Vector Laboratories). Analysis was done using a Zeiss LSM 510 META confocal multiphoton microscope system under UV excitation at 488 nm (for AlexaFluor^{488}), 630 nm (for Cy5), 540 nm (for rhodamine), and 340 nm (for DAPI). Protein colocalization was estimated by calculating the area of color overlap in a Z-stack of images using MetaMorph software.

Solid-phase adhesion assays. Exponentially growing cells were detached from culture plates by trypsinization and labeled with calcein acetoxymethylester (calcein AM; 2 μmol/L; Molecular Probes) for 20 min. After washing, cells were resuspended in serum-free medium. Equal numbers of cells (4×10^4 per well) were seeded into 96-well plates precoated with fibronectin (Sigma) at different concentrations (1–10 μg/mL) or bovine serum albumin (1% w/v). After 1 h of incubation at 37°C, the plate was immersed into PBS containing 1 mmol/L $MgCl_2$ to remove nonadherent cells. The number of adherent cells was measured in a fluorescence plate reader (Applied Biosystems) at an excitation wavelength of 485 nm and an emission wavelength of 530 nm. All experiments were done in quadruplicate and repeated twice.

Cell migration assays. A migration assay was done in a modified Boyden chamber method using 6.5-mm-diameter, 8.0-μm pore size polycarbonate membrane transwell inserts in a 24-well plate (Corning). To assess directional migration, the lower surfaces of the transwell membrane were coated with 50 μg/mL fibronectin or with 0.01% type I collagen (Sigma). SKOV3 cells stably transfected with AS-TG2 or vector were serum starved for 18 h and then plated in the upper well at a concentration of 2×10^5 in 100 μL of serum-free medium. After 4 h of incubation at 37°C in a CO_2 incubator, the cells on the upper surface of the membrane were wiped off with a cotton swab. The cells on the lower surface of the transwell were stained with HEMA3 stain (Fisher) and counted at ×200 magnification. Cells were counted in five high-power fields (HPF) in duplicate experiments. Results are expressed as mean number of migrating cells ± SE. A similar experiment was done using serum-free conditioned medium from cells stably transfected with AS-TG2 or pcDNA3.1 as cell attractant in the lower chamber of the transwell.

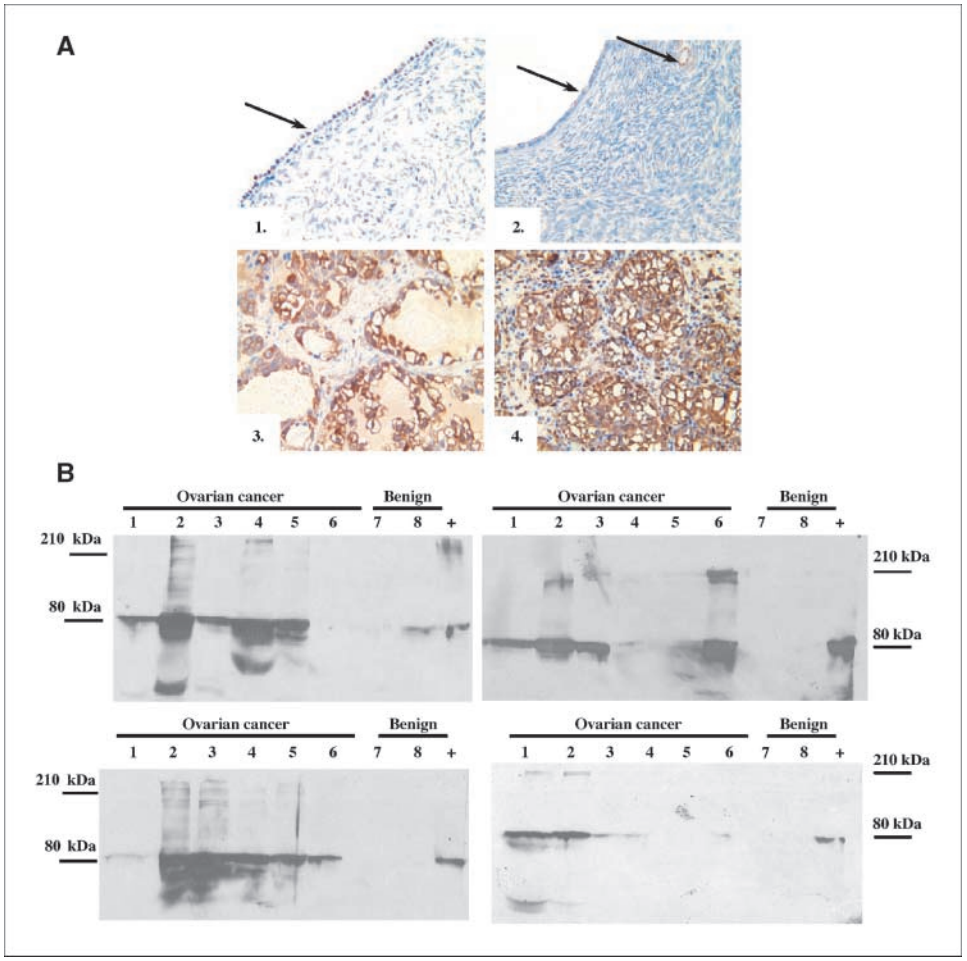

Figure 1. *A,* expression of TG2 by immunohistochemistry in ovarian tumors and normal ovary. *1* and *2,* normal ovary. Arrows point to normal ovarian epithelium and to a surface epithelial inclusion. *3* and *4,* representative ovarian tumors. *B,* TG2 expression in ascites specimens. Each immunoblot includes six specimens of malignant ascites from patients with EOC (*lanes 1–6*), two specimens of ascites fluid or pleural fluid from patients with nonmalignant diseases (*lanes 7* and *8*), and a positive control (lysate from ovarian cancer cell line, SKOV3). Equal volume (30 μL) of ascites fluid was loaded in each lane.

***In vivo* growth of SKOV3 cells in nude mice.** The human ovarian cancer cell line SKOV3 stably transfected with AS-TG2 or vector was injected i.p. into 7- to 8-week-old female nude mice (*nu/nu* BALB/c) from Harlan. Eight weeks after the injection, the mice were euthanized and a necropsy was done. Tumor formation was estimated by two methods. First, we measured bidimensionally tumors >0.4 cm with calipers and calculated tumor volume according to the formula $L \times W^2 / 2$, where L is length and W is width. A cumulative tumor volume was calculated by adding the volumes of dominant tumors for each animal. Second, we estimated peritoneal seeding with unmeasurable 1- to 3-mm tumors by counting the number of implants on the mesentery, omentum, and peritoneum. Harvested tumors were preserved in formalin for future histologic and immunohistochemical studies. When possible, tumors were minced and cultured in medium supplemented with G418 in the presence of hyaluronidase at a concentration of 1 mg/mL. The xenograft-derived cultures were characterized by immunoblotting and solid-phase assay. Animal experiments were approved by the Indiana University School of Medicine Animal Care and Use Committee (protocol 2680) and were in accordance with federal regulations. Three independent experiments were done.

Flow cytometry. Quantification of cell surface β_1 integrin was done using the FACScan/CellQuest system (Becton Dickinson). Trypsinized cells were incubated with β_1 integrin monoclonal antibody (1:100 dilution) or mouse IgG for 1 h on ice. After incubation with secondary AlexaFluor^{488}-labeled anti-mouse IgG (1:500 dilution), immunofluorescent staining was quantified using the FACScan/CellQuest system. Ten thousand events were accumulated for each analysis. Three independent readings were obtained from separate experiments, and data were averaged for statistical analysis.

Statistical analysis. For the analysis of the immunohistochemical and immunoblotting data in cancer and noncancer specimens, the χ^2 test was used. Likewise, the χ^2 was used for the comparison between animals developing peritoneal studding in the groups injected with AS-TG2–transfected or control cells. For the solid-phase adhesion and migration assays, flow cytometry analysis, and comparison of volumes and number of peritoneal implants between the two animal groups, we used the Student's t test.

Results

TG2 is expressed in EOC. We used immunohistochemical assay to determine expression of TG2 in ovarian tumors. Among 27 tumors, we found intense cytoplasmic and membrane staining (2 to 3+) in 21 specimens (79% of tumors; Fig. 1*A*). Two specimens stained weakly (1+) and four tumors did not stain. All histologic subtypes were immunoreactive: 9 of 9 clear cell carcinoma were intensely positive, 3 of 3 endometrioid tumors displayed 2+ staining, and 9 of 14 papillary serous tumors were 2 to 3+ positive. One poorly differentiated carcinoma did not immunoreact. Details of tumor characteristics, including stage, histologic type, and grade, are included in Supplementary Table S1. TG2 expression was noted in advanced tumors (10 of 13 stage III and IV tumors) as well as in early-stage disease (13 of 14 stage I and II tumors). In normal ovary, TG2 immunoreactivity was weak in normal stroma and absent in the surface epithelial layer. None of six normal ovarian specimens immunostained for TG2 in the epithelium, suggesting that TG2

expression is specific to transformed ovarian epithelial cells (P = 0.005), but weak staining was observed in surface epithelial inclusions (Fig. 1*A*). Control staining (without primary antibody) was consistently negative.

TG2 is secreted in EOC malignant ascites. Because ovarian cancer disseminates in the peritoneal cavity, large volumes of ascites that contain proteins secreted by tumor and mesothelial cells are generated (22). Such secreted proteins modulate the growth and spread of carcinoma cells in the peritoneal milieu (9, 23, 24). Knowing that TG2 is a secreted protein, we tested whether it is detectable in ascites. Immunoblot analysis revealed the presence of TG2 in 25 of 30 ascites specimens from patients with EOC (representative immunoblots illustrated in Fig. 1*B*). There was variable level of TG2 secretion among the malignant ascites specimens. Eight specimens of nonmalignant, inflammatory effusions contained none or negligible TG2 (one of eight samples), suggesting that TG2 secretion is specific to cancer cells (P = 0.005). Immunoblot analysis revealed a higher molecular weight band, migrating at ~170 kDa in several ascites specimens. This was also observed in conditioned medium from some of the ovarian cancer cell lines (data not shown) and was partially disrupted by stringent denaturing conditions (SDS or 2-mercapthoethanol), suggesting that

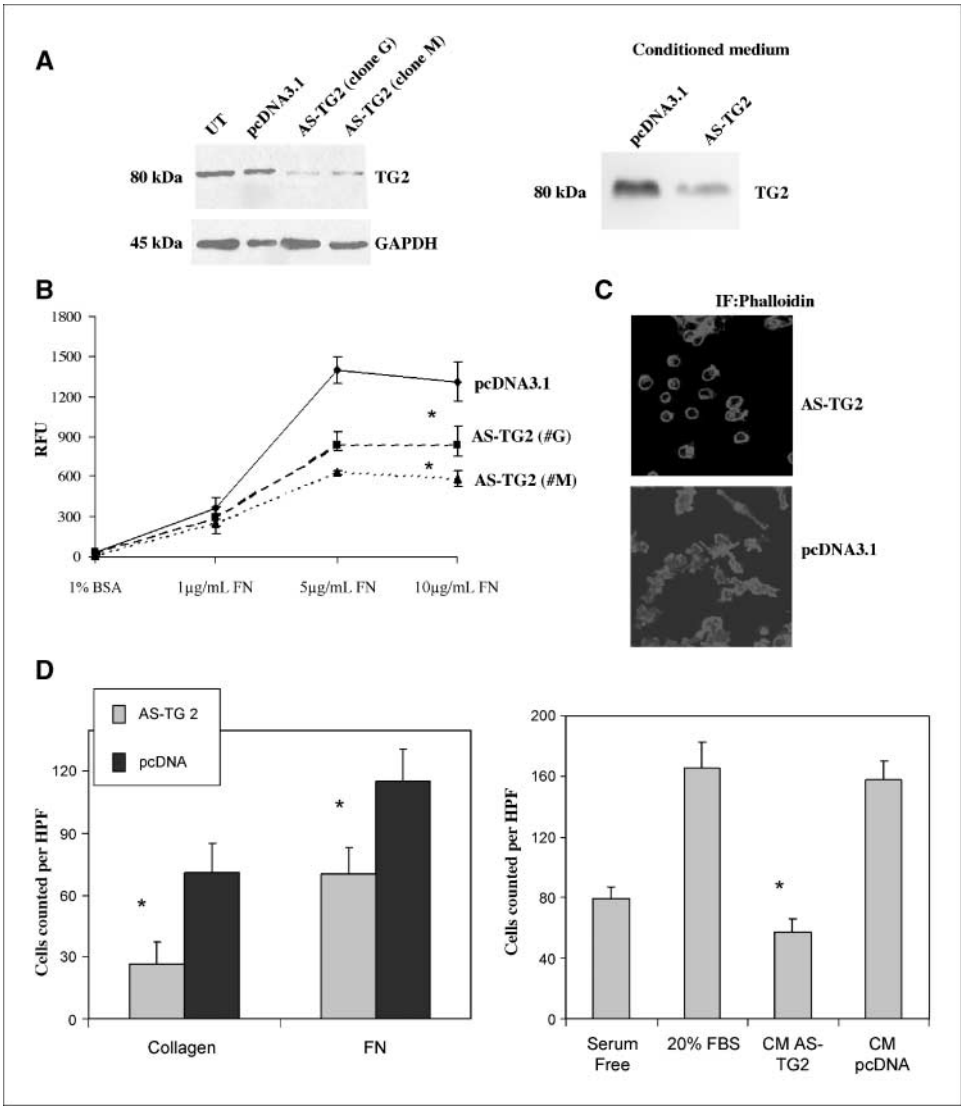

Figure 2. Effects of TG2 knockdown on ovarian cancer cell adhesion and migration. *A,* Western blot analysis for TG2 using cell lysates and conditioned medium. G and M are stable clones identified by selection with G418 after transfection with AS-TG2. Controls are untransfected cells (*UT*) and cells stably transfected with pcDNA3.1. Serum-free conditioned medium from AS-TG2 clone (G) was compared with conditioned medium from pcDNA3.1-transfected cells by immunoblotting. Equal volume of conditioned medium was loaded in each lane (30 μL). *B,* solid-phase assay measured adhesion to fibronectin (*FN*) for vector-transfected and AS-TG2–transfected cells. Number of cells adhering to fibronectin within 1 h was quantified based on fluorescence emission after cells were labeled with calcein AM [relative fluorescence units (*RFU*)]. *Points,* mean of four replicates; *bars,* SE. P = 0.006. *BSA,* bovine serum albumin. *C,* staining for phalloidin in SKOV3 cells stably transfected with AS-TG2 or vector. Cells were plated on fibronectin-coated coverslips, allowed to adhere for 60 min, and then fixed and stained with rhodamine-phalloidin antibody. *Red signal,* visualization was done under UV excitation at 520 nm with a confocal microscope. *D,* effects of TG2 on directional cell migration. *Left,* directional migration stimulated by collagen or fibronectin as measured in SKOV3 cells stably transfected with AS-TG2 or pcDNA3.1 by transwell assay. Cells (1×10^6) were plated in each well. Cells migrating to the lower surface of the filter within 5 h were counted. *Columns,* average of cells counted per 10 HPF for each experimental condition; *bars,* SE. $P < 0.001$. *Right,* directional migration stimulated by fibronectin and conditioned medium (*CM*) in SKOV3 cells. SKOV3 cells (1×10^6) were plated in each well. In the lower chamber, the medium consisted of serum-free medium (negative control; *first column*), medium with 20% FBS (positive control; *second column*), and serum-free conditioned medium collected from SKOV3 cells stably transfected with AS-TG2 (*third column*) or pcDNA3.1 (*fourth column*). Cells migrating to the lower surface of the filter within 5 h were counted. *Columns,* average of cells counted per 10 HPF; *bars,* SE. $P < 0.001$.

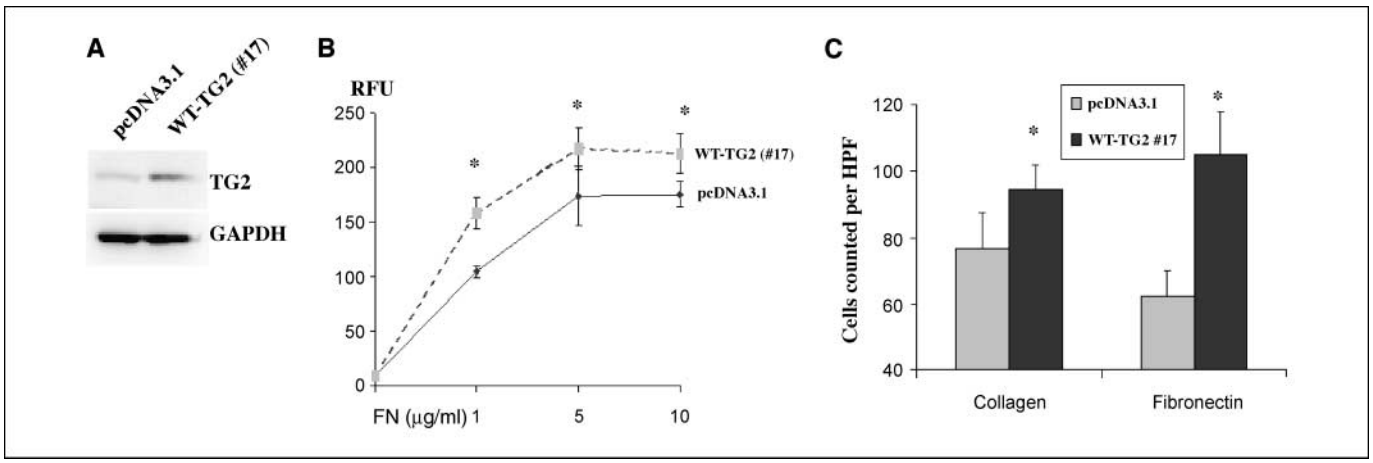

Figure 3. Effects of TG2 overexpression on ovarian cancer cell adhesion and directional migration. *A,* Western blot analysis for TG2. OV90 cells transfected with TG2 or pcDNA3.1 vector were selected with G418. Western blot analysis for TG2 identifies clone 17 as a stable clone expressing TG2. *B,* solid-phase assay measured adhesion to fibronectin for cells stably transfected with TG2 or pcDNA3.1. *Points,* mean of four replicates; *bars,* SE. $P = 0.01$. *C,* directional migration stimulated by collagen or fibronectin was measured in OV90 cells stably transfected with TG2 or pcDNA3.1. Cells (1×10^6) were plated in each well. Cells migrating to the lower surface of the filter within 5 h were counted. *Columns,* average of cells counted per 10 HPF; *bars,* SE. $P < 0.001$.

it represents a covalently linked dimer. These data suggest that TG2 is up-regulated in EOC cells and secreted in malignant ascites.

TG2 facilitates ovarian cancer cell adhesion to fibronectin and directional cell migration. To understand the function of TG2 in ovarian cancer cells, we generated stable human cell lines, in which TG2 was overexpressed or knocked down. To knock down TG2, we used an antisense construct (AS-TG2) cloned in pcDNA3.1 (25) in SKOV3 ovarian cancer cells, which expresses abundant TG2. Two stable clones (G and M) were selected based on G418 resistance and screening by immunoblotting. Decreased TG2 was noted in whole-cell lysates and conditioned medium from these clones compared with vector-transfected cells (Fig. 2*A*).

Next, we wished to determine whether TG2 mediated ovarian cancer cell dissemination in the peritoneal space and examined its involvement in cell adhesion and directional migration. Using a solid-phase assay, we found that stable knockdown of TG2 in SKOV3 cells decreased ovarian cancer cell adhesion to fibronectin by >50% at all concentrations of fibronectin tested compared with control cells (Fig. 2*B*). Cell spread on fibronectin was visualized by staining the cytoskeleton with rhodamine-phalloidin. AS-TG2–transfected cells were round and failed to extend lamellipodia, whereas cells transfected with vector spread readily on fibronectin (Fig. 2*C*).

The effects of TG2 on directional cell migration were measured by a transwell assay. Fibronectin- and collagen-stimulated chemotaxis was decreased in SKOV3 cells stably transfected with AS-TG2 compared with cells transfected with vector (Fig. 2*D*). In addition, secreted TG2 acted as an attractant, stimulating ovarian cancer cell migration across the transwell. Directional cell migration of SKOV3 cells induced by conditioned medium was significantly lower when the assay was done with conditioned medium lacking TG2 (from AS-TG2 cells) compared with conditioned medium from control cells (Fig. 2*D*).

Next, we tested whether stable overexpression of TG2 increases adhesion to fibronectin. For this, an ovarian cancer cell line with low endogenous TG2 (OV90) was transfected with TG2. A stably transfected clone was identified by immunoblotting after selection with G418 (Fig. 3*A*). Stable expression of TG2 enhanced adhesion to fibronectin compared with cells transfected with empty vector (Fig. 3*B*). Likewise, directional cell migration stimulated by fibronectin or collagen was enhanced by stable expression of TG2 (Fig. 3*C*). Coupled with the effects of TG2 knockdown, these experiments show that TG2 is critical to ovarian cancer cell adhesion and directional migration, essential steps in metastasis.

TG2 knockdown inhibits tumor development and spread on the peritoneal surface *in vivo*. We injected nude mice i.p. with SKOV3 cells stably transfected with AS-TG2 or empty vector, and after 8 weeks, we observed a significant difference in pattern of tumor development. Mice injected with pcDNA3.1-transfected (empty vector) cells developed tumors in the omentum and the retroperitoneal space and numerous 1- to 3-mm tumors studding the mesentery adjacent to the bowel and on the peritoneal surface of abdominal flanks (Fig. 4*A* and *B*). The average number of

Table 1. Tumor formation in the peritoneal space according to TG2 expression

		pcDNA3.1	AS-TG2	*P*
Experiment 1	No. mice	5	6	
	Volume (mm^3)*	268 ± 33	214 ± 40	0.392
	No. implants	81 ± 11	10.5 ± 4.3	0.0002 †
Experiment 2	No. mice	5	5	
	Volume (mm^3)*	172 ± 70	342 ± 90	0.392
	No. implants	65.8 ± 12	14.6 ± 5.4	0.005 †
Experiment 3	No. mice	4	6	
	Volume (mm^3)*	1152 ± 394	369 ± 83	0.139
	No. implants	81.5 ± 23	24 ± 18	0.09
Combined	No. mice	14	17	
	Volume (mm^3)*	486 ± 130	306 ± 44	0.288
	No. implants	76 ± 8	17 ± 6	0.00001 †

NOTE: Data are presented as average volume and average number of implants ± SE.
* Tumor volume was calculated by adding the volume of individual tumors >0.4 cm in greatest dimension for each animal.
† Statistically significant.

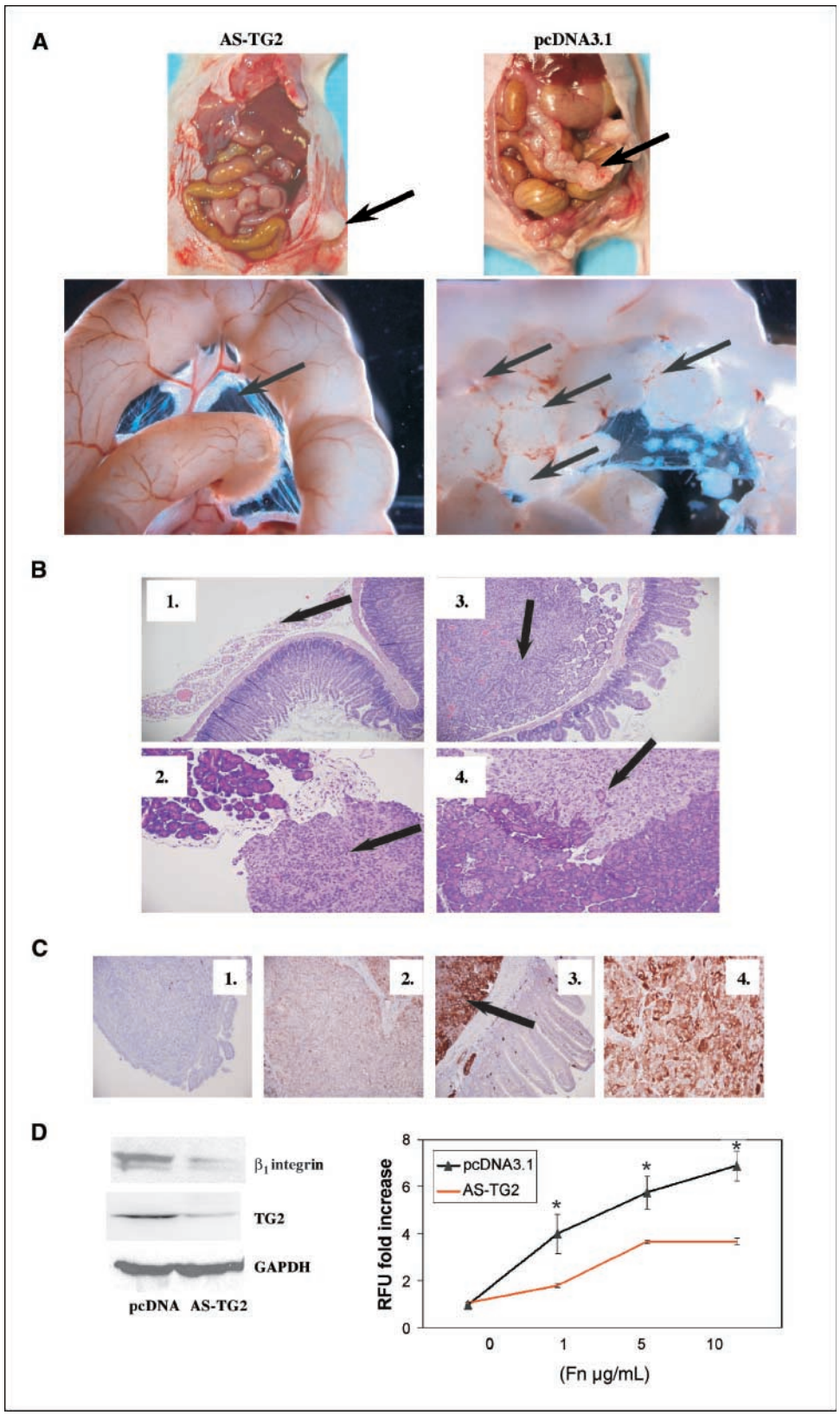

Figure 4. TG2 knockdown inhibits tumor development and i.p. dissemination *in vivo*. *A, in vivo* tumor development. Nude mice injected with control cells (pcDNA3.1-SKOV3) form tumors studding the mesentery and peritoneal surface as well as tumors infiltrating the retroperitoneal space. Mice injected with AS-TG2–transfected cells form tumors in the retroperitoneal space, at the site of the i.p. injection, and have clear mesentery. The images of open animals provide a direct view of the small bowel and mesentery. In the animal injected with pcDNA3.1-transfected cells, arrow points to large tumors on the mesentery adjacent to the small bowel. In the mouse injected with AS-TG2 cells, arrow points to tumor nodule at the site of i.p injection. Macroscopically, the bowel and mesentery appear clear. Pieces of small bowel and adjacent mesentery were photographed at ×12 magnification with a Stemi SV11 Apo Zeiss dissecting microscope. In the mouse injected with AS-TG2 cells, the arrow points to clear mesentery. In the animal injected with control cells, the multiple arrows indicate many tumor implants studding the mesentery. *B,* histologic appearance of xenografts (H&E staining). *1,* no tumor is visualized on the mesentery in animals injected with AS-TG2 cells; *3,* block of tumor derived from pcDNA3.1-SKOV3 cells invading the mesentery adjacent to bowel; *2* and *4,* AS-TG2–derived and pcDNA3.1-derived tumor infiltrating the pancreas. Arrows point to tumor deposits in sections 2, 3, and 4. In section 1, arrow points to clear mesentery adjacent to normal bowel. *C,* expression of TG2 by immunohistochemistry in xenografts. *1,* negative control (no primary antibody, pcDNA3.1-derived tumor); *2,* TG2 staining is absent in tumors derived from AS-TG2 cells; *3* and *4,* intense TG2 staining noted in tumors derived from pcDNA3.1-transfected SKOV3 cells. *3, arrow,* a peritoneal implant in the mesentery adjacent to normal bowel. *D,* characteristics of xenograft-derived cell cultures. Expression of TG2 and β_1 integrin assessed by immunoblotting is diminished in cultures derived from AS-TG2 xenografts compared with controls (pcDNA3.1 xenografts). Adhesion to fibronectin, as measured by solid-phase assay, is also diminished in cells derived from AS-TG2 xenografts compared with controls. Fold difference in measured fluorescence (relative fluorescence units) corresponding to the number of cells adherent within 1 h to fibronectin-coated surfaces. Fibronectin concentrations varied between 1 and 10 μg/mL.

implants was 76 ± 8. Mice injected with AS-TG2–transfected cells developed one large tumor in the omentum, invading into the retroperitoneal space, and a tumor nodule at the injection site, but significantly fewer mesenteric implants (17 ± 6; Table 1). The tumor volume of dominant masses was not significantly different for AS-TG2–derived xenografts compared with controls (Table 1). Twelve of 14 mice injected with control cells developed milliary peritoneal metastases, whereas only 2 of 17 mice injected with

AS-TG2 cells developed milliary studding of the mesentery ($P < 0.0001$; Supplementary Table S2). Tumors were of similar histologic appearance, with high nuclear grade for both groups, and a serous papillary pattern was discernible in mesenteric implants.

TG2 knockdown was retained *in vivo* as shown by immunohistochemistry in xenografts and by Western blot analysis of cell cultures established from explanted xenografts (Fig. 4*C* and *D*). Occasional small and isolated islands of TG2-positive cells were observed in tumors from AS-TG2 cells, consistent with the emergence of some TG2-positive subpopulations in the absence of G418 selection *in vivo*. However, general preservation of the TG2 knockdown *in vivo* is shown by the observation that cell cultures from explanted xenografts conserved their original phenotype (Fig. 4*D*). In addition, decreased adhesion to fibronectin was noted between cells cultured from AS-TG2 and control tumors. The pattern of tumor formation in the peritoneal space was consistent with the phenotype observed *in vitro*, suggesting an important role for TG2 in peritoneal studding.

TG2 interacts with β_1 integrin and modulates its expression. As alteration in the level of TG2 expression modulates EOC cell adhesion *in vitro* and *in vivo*, we examined whether TG2 interacts with integrins. Knowing that β_1 integrin has been linked to invasion and metastasis in EOC (26), we evaluated interaction of TG2 with this subunit. Immunoprecipitation with β_1 integrin antibody followed by immunoblotting for TG2 shows endogenous interaction between TG2 and β_1 integrin in EOC cells. TG2 and β_1 integrin also colocalized in cytoplasmic organelles (Fig. 5*A*). We also examined the level of β_1 integrin in cells with diminished TG2 expression and found that the β_1 subunit is expressed at decreased levels in AS-TG2–transfected cells (Fig. 5*B*). However, *mRNA* levels were not different between AS-TG2 and control cells, suggesting that TG2 affects integrin processing posttranscriptionally. Decreased β_1 subunit in the plasma membrane fraction was confirmed by Western blotting in SKOV3 transfected with AS-TG2 compared with controls. Expression of β_1 integrin on the cell surface was estimated by fluorescence-activated cell sorting (FACS) and immunofluorescent staining. FACS analysis revealed reduced levels of β_1 integrin on the surface of AS-TG2 cells compared with controls (Fig. 5*C*). In cells expressing AS-TG2, immunofluorescence also showed reduced distribution of β_1 integrin to the cell membrane (Fig. 5*D*).

To measure whether changes in rates of protein degradation contribute to the difference in β_1 integrin expression dependent on the TG2 status of ovarian cancer cells, we treated AS-TG2 and control cells with cycloheximide and measured β_1 integrin levels by immunoblotting. In AS-TG2 cells, β_1 integrin was degraded more rapidly [half-life ($t_{1/2}$) = 3–6 h] compared with control cells ($t_{1/2}$ = 12–24 h; Supplementary Fig. S1*A*). To assess lysosomal-, ubiquitin-, or calpain-mediated β_1 integrin proteolysis in AS-TG2 or pcDNA3.1-transfected (vector) ovarian cancer cells, we measured integrin levels by immunoblotting after incubating cells

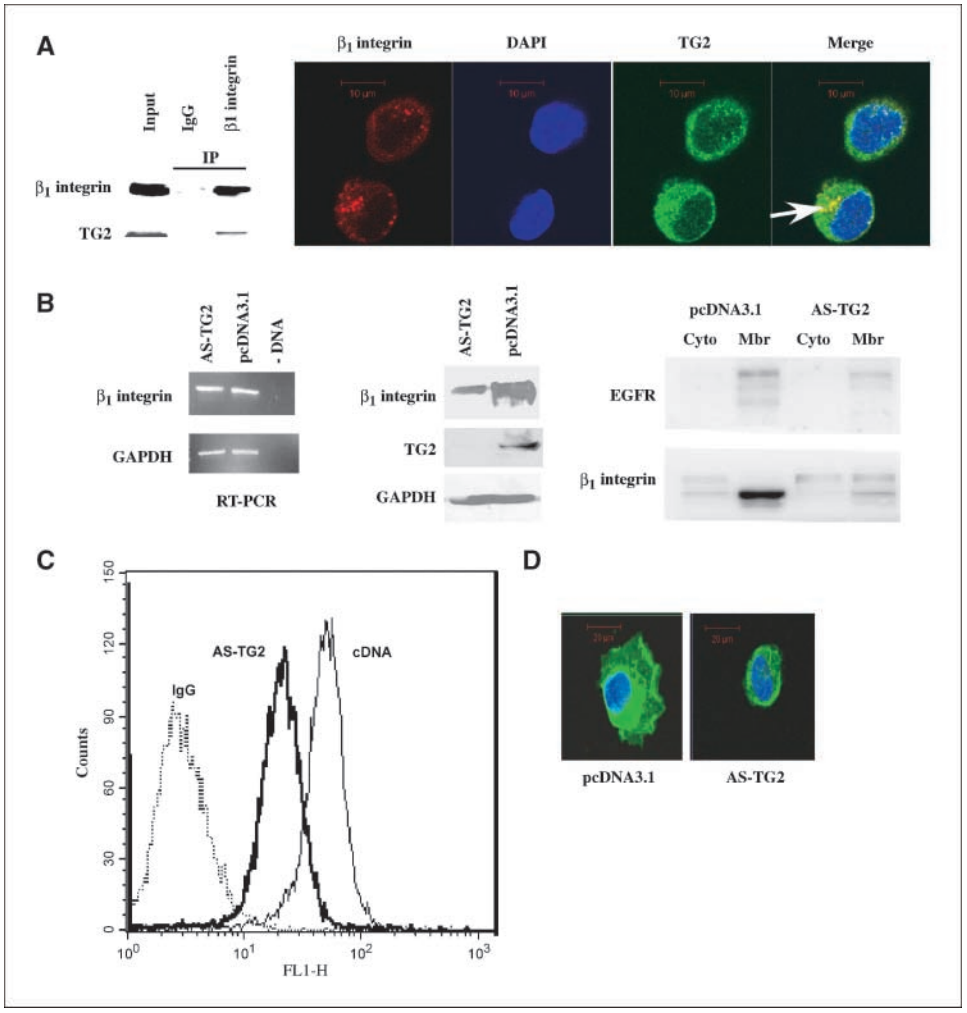

Figure 5. Interaction and correlation between TG2 and β_1 integrin. *A,* interaction between TG2 and β_1 integrin. Immunoprecipitation (*IP*) was carried out with monoclonal anti-β_1 integrin antibody or IgG and Western blot analysis using anti-TG2 antibody. *Input,* 50 μg of cell lysate. Immunofluorescence with polyclonal anti-TG2 antibody (secondary antibody labeled with AlexaFluor^{488}; *green*) and a monoclonal anti-β_1 integrin antibody (secondary antibody labeled with Cy5; *red*) was used to identify cellular localization of the two proteins. Protein colocalization is identified by emergence of yellow spectra on merged images and was quantified by using the MetaMorph software in a Z-stack of images. Sixty-four percent of β_1 integrin colocalized with TG2. Nuclei were visualized by DAPI staining. *B,* down-regulation of TG2 in ovarian cancer cells correlates with decreased β_1 integrin expression at protein level and its presentation to the cell membrane. TG2 and β_1 integrin expression were measured in cells stably transfected with AS-TG2 and pcDNA3.1 by RT-PCR (*mRNA* level; *right*), immunoblotting (protein level; *middle*), and cell fractionation followed by immunoblotting (*left*). Blotting for EGFR was used as control for the membrane fractions. *C,* FACS analysis for β_1 integrin in cells stably transfected with pcDNA3.1 or AS-TG2. Mean fluorescent intensity values were 2.9 for IgG (negative control), 20.1 for AS-TG2 cells, and 47 for pcDNA3.1-transfected cells. *D,* immunofluorescent staining for β_1 integrin (secondary antibody labeled with AlexaFluor^{488}; *green*) in cells stably transfected with pcDNA3.1 or AS-TG2.

with lysosomal inhibitor (leupeptin), proteasomal inhibitors (MG132 and lactacystin), calpain inhibitor (PD105606), and protein trafficking inhibitors (monensin and chloroquine). Treatment with the proteasomal inhibitor MG132, and more prominently with the calpain inhibitor PD105606, restored β_1 integrin levels in AS-TG2 cells (Supplementary Fig. S1*B–D*), suggesting that TG2 interferes with calpain-mediated β_1 integrin degradation in EOC cells. In contrast, inhibition of lysosomal proteases (leupeptin) did not significantly alter integrin levels in AS-TG2 cells (Supplementary Fig. S1*E*). These observations may explain the selective down-regulation of β_1 integrin levels in cells transfected with AS-TG2 and identify a novel function of TG2 in epithelial cancer cells.

Discussion

I.p. metastasis characteristic of EOC requires modifications of tumor cells to facilitate interaction with the peritoneal stroma and mesothelium. In this report, we show overexpression of TG2 in ovarian tumors and its secretion in malignant ascites fluid. We show that TG2 mediates ovarian cancer cell adhesion to fibronectin and stimulates directional cell motility, these processes being mediated by TG2 via interaction and stabilization of β_1 integrin. Using an i.p. xenograft model, we show that TG2 knockdown decreases the pattern of diffuse tumor spread, implicating it as a mediator of i.p. metastasis.

Having identified TG2 as an overexpressed transcript in primary EOC cells (15), we show here that >75% of ovarian tumors overexpress the protein. TG2 is not expressed on the surface ovarian epithelium but is present in stage I and II ovarian tumors. TG2 up-regulation has been reported in glioblastoma, pancreatic, breast, and lung cancer, and a multitude of functions has been invoked for it (21, 27, 28). We focus here on the induced stabilization of cell adhesion of TG2, as this is critical to the establishment of i.p. metastases, where cancer cells are required to "stick" to the oncomatrix to establish peritoneal implants. Adhesion to fibronectin and chemotaxis was decreased in EOC cells by knockdown of TG2 and enhanced by stable overexpression of the protein. This phenotype was preserved *in vivo*, where the pattern of distribution of i.p. implants was altered by TG2 knockdown. Control animals injected with SKOV3-pcDNA3.1 cells developed i.p. implants widely disseminated on the mesentery and the peritoneal/hepatic gutters, resembling the human disease. Animals injected with SKOV3/AS-TG2 cells developed large tumors in the retroperitoneal space and few or no mesenteric metastatic foci, suggesting that TG2 plays an important role in mediating development of peritoneal metastases. The volume of dominant masses was not significantly different in animals injected with AS-TG2 cells compared with controls, whereas peritoneal seeding was considerably decreased (Fig. 4; Table 1; Supplementary Table S2). An association between TG2 and an invasive clinical phenotype was recently described for pancreatic cancer, activation of focal adhesion kinase being considered the main involved mechanism (17). Other functions of the enzyme, and especially its protective role against apoptosis, shown in other systems, might also play a role (27–30).

The altered metastatic phenotype observed by us is due to deficient interaction between tumor cells and the ECM in the absence of TG2. It has been previously shown that TG2 in complex with β_1 integrin enhances cell adhesion to fibronectin (31) and that TG2 interacts directly with the 42-kDa domain of fibronectin, consisting of modules I_6 $II_{1,2}$ I_{7-9} (31, 32). We have observed interaction of TG2 and β_1 integrin in cells, but interestingly, TG2 and β_1 integrin do not interact *in vitro* (33). Our unpublished observations also show that addition of exogenous TG2 (recombinant TG2 or protein purified from guinea pig liver) fails to increase ovarian cancer cell adhesion to fibronectin, suggesting that the mere presence of TG2 in the extracellular milieu is not sufficient to facilitate cell adhesion. Interestingly, we found diminished expression of β_1 integrin subunit on the surface of cells where TG2 was stably down-regulated. Further, degradation of β_1 integrin was more rapid in AS-TG2 cells compared with controls and inhibition of calpain-mediated integrin degradation, but not of lysosomal proteases, restored its expression level. These observations suggest that, in the absence of TG2, β_1 integrin is cleared rapidly via calpain-induced proteolysis. These data highlight a novel function for transglutaminase, distinct from its previously suggested role as a "coreceptor" for fibronectin (33). As β_1 integrin can complex several α subunits, modulating cell-matrix interactions, TG2 down-regulation may affect integrin complex formation, leading to deficient cell adhesion to different components of the ECM. By directly modulating integrin expression, TG2 could affect the invasiveness of ovarian tumors and clinical outcome (26, 34, 35) as well as sensitivity to chemotherapy (36–38). Integrin signaling has been linked to cancer metastasis (39–41), and disruption of integrin function by competing antibodies or peptides has been proposed as a possible cancer treatment (42–44). The data presented here provide compelling evidence that TG2 may be a target, as its interaction with and regulation of integrins directly promote cell adhesion, which is an important step in peritoneal metastasis.

We also found that TG2 is secreted abundantly in malignant ascites fluid. This is likely due to accumulation from tumor and/or mesothelial cells, as primary ovarian cancer cells and cancer cell lines secrete TG2. Although TG2 lacks a leader sequence, it is secreted into the extracellular space through an as yet unknown mechanism (45). The expression of TG2 in tumor cells supports its detection in ascites fluid. We cannot exclude the contribution of mesothelial cells to the composition of malignant ascites; however, the absence of TG2 in inflammatory ascites of pleural fluid makes it likely that TG2 is secreted directly by the tumor cells. Other factors critical to i.p. metastasis are secreted abundantly in ascites, fibronectin, lysophosphatidic acid, hyaluran, and vascular endothelial growth factor, making the i.p. milieu favorable for cancer cell growth (11, 46). The presence of TG2 in the peritoneal fluid may play a role in remodeling the oncomatrix by cross-linking of ECM proteins.

The important conclusion of this study is that TG2 is highly expressed in human ovarian tumor cells and is secreted in malignant ascites. At the interface between cancer cells and the stroma, TG2 alters the pattern of tumor growth and dissemination in the peritoneal space by modulating β_1 integrin expression and function.

Acknowledgments

Received 1/24/2007; revised 4/14/2007; accepted 5/24/2007.

Grant support: American Cancer Society grants IRG-84-002-19 and MRSG 107613, Indiana University Cancer Center Ovarian Cancer Pilot Grant, Showalter Research Fund, and Marsha Rivkin (D. Matei).

The costs of publication of this article were defrayed in part by the payment of page charges. This article must therefore be hereby marked *advertisement* in accordance with 18 U.S.C. Section 1734 solely to indicate this fact.

We thank Dr. David Donner (University of California at San Francisco, San Francisco, CA) for helpful advice and critical review of the manuscript, Dr. Janusz Tucholski (University of Alabama) for plasmids, and Dr. Jyianou Rao (University of California at Los Angeles, Los Angeles, CA) for ascites specimens.

References

1. Auersperg N, Wong AS, Choi KC, Kang SK, Leung PC. Ovarian surface epithelium: biology, endocrinology, and pathology. Endocr Rev 2001;22:255–88.
2. Auersperg N, Pan J, Grove BD, et al. E-cadherin induces mesenchymal-to-epithelial transition in human ovarian surface epithelium. Proc Natl Acad Sci U S A 1999;96:6249–54.
3. Davidson B, Goldberg I, Reich R, et al. α_V- and β_1-integrin subunits are commonly expressed in malignant effusions from ovarian carcinoma patients. Gynecol Oncol 2003;90:248–57.
4. Gardner MJ, Jones LM, Catterall JB, Turner GA. Expression of cell adhesion molecules on ovarian tumour cell lines and mesothelial cells, in relation to ovarian cancer metastasis. Cancer Lett 1995;91:229–34.
5. Ahmed N, Pansino F, Clyde R, et al. Overexpression of $\alpha(v)\beta_6$ integrin in serous epithelial ovarian cancer regulates extracellular matrix degradation via the plasminogen activation cascade. Carcinogenesis 2002; 23:237–44.
6. Cruet-Hennequart S, Maubant S, Luis J, Gauduchon P, Staedel C, Dedhar S. $\alpha(v)$ integrins regulate cell proliferation through integrin-linked kinase (ILK) in ovarian cancer cells. Oncogene 2003;22:1688–702.
7. Casey RC, Skubitz AP. CD44 and β_1 integrins mediate ovarian carcinoma cell migration toward extracellular matrix proteins. Clin Exp Metastasis 2000;18:67–75.
8. Scotton CJ, Wilson JL, Milliken D, Stamp G, Balkwill FR. Epithelial cancer cell migration: a role for chemokine receptors? Cancer Res 2001;61:4961–5.
9. Xu Y, Gaudette DC, Boynton JD, et al. Characterization of an ovarian cancer activating factor in ascites from ovarian cancer patients. Clin Cancer Res 1995;1:1223–32.
10. Carreiras F, Cruet S, Staedel C, Sichel F, Gauduchon P. Human ovarian adenocarcinoma cells synthesize vitronectin and use it to organize their adhesion. Gynecol Oncol 1999;72:312–22.
11. Byers LJ, Osborne JL, Carson LF, et al. Increased levels of laminin in ascitic fluid of patients with ovarian cancer. Cancer Lett 1995;88:67–72.
12. Gillan L, Matei D, Fishman DA, Gerbin CS, Karlan BY, Chang DD. Periostin secreted by epithelial ovarian carcinoma is a ligand for $\alpha(V)\beta(3)$ and $\alpha(V)\beta(5)$ integrins and promotes cell motility. Cancer Res 2002;62:5358–64.
13. Morales CP, Holt SE, Ouellette M, et al. Absence of cancer-associated changes in human fibroblasts immortalized with telomerase. Nat Genet 1999;21:115–8.
14. Buczek-Thomas JA, Chen N, Hasan T. Integrin-mediated adhesion and signalling in ovarian cancer cells. Cell Signal 1998;10:55–63.
15. Matei D, Graeber TG, Baldwin RL, Karlan BY, Rao J, Chang DD. Gene expression in epithelial ovarian carcinoma. Oncogene 2002;21:6289–98.
16. Grigoriev MY, Suspitsin EN, Togo AV, et al. Tissue transglutaminase expression in breast carcinomas. J Exp Clin Cancer Res 2001;20:265–8.
17. Verma A, Wang H, Manavathi B, et al. Increased expression of tissue transglutaminase in pancreatic ductal adenocarcinoma and its implications in drug resistance and metastasis. Cancer Res 2006;66:10525–33.
18. Martinet N, Bonnard L, Regnault V, et al. *In vivo* transglutaminase type 1 expression in normal lung, preinvasive bronchial lesions, and lung cancer. Am J Respir Cell Mol Biol 2003;28:428–35.
19. Mishra S, Murphy LJ. Tissue transglutaminase has intrinsic kinase activity: identification of transglutaminase 2 as an insulin-like growth factor-binding protein-3 kinase. J Biol Chem 2004;279:23863–8.
20. Mehta K, Lopez-Berestein G, Moore WT, Davies PJ. Interferon-γ requires serum retinoids to promote the expression of tissue transglutaminase in cultured human blood monocytes. J Immunol 1985;134:2053–6.
21. Herman JF, Mangala LS, Mehta K. Implications of increased tissue transglutaminase (TG2) expression in drug-resistant breast cancer (MCF-7) cells. Oncogene 2006;25:3049–58.
22. Richardson M, Gunawan J, Hatton MW, Seidlitz E, Hirte HW, Singh G. Malignant ascites fluid (MAF), including ovarian-cancer-associated MAF, contains angiostatin and other factor(s) which inhibit angiogenesis. Gynecol Oncol 2002;86:279–87.
23. Graves LE, Ariztia EV, Navari JR, Matzel HJ, Stack MS, Fishman DA. Proinvasive properties of ovarian cancer ascites-derived membrane vesicles. Cancer Res 2004;64: 7045–9.
24. Xu Y, Shen Z, Wiper DW, et al. Lysophosphatidic acid as a potential biomarker for ovarian and other gynecologic cancers. JAMA 1998;280:719–23.
25. Tucholski J, Lesort M, Johnson GV. Tissue transglutaminase is essential for neurite outgrowth in human neuroblastoma SH-SY5Y cells. Neuroscience 2001;102:481–91.
26. Arboleda MJ, Lyons JF, Kabbinavar FF, et al. Overexpression of AKT2/protein kinase Bβ leads to up-regulation of β_1 integrins, increased invasion, and metastasis of human breast and ovarian cancer cells. Cancer Res 2003;63:196–206.
27. Yuan L, Choi K, Khosla C, et al. Tissue transglutaminase 2 inhibition promotes cell death and chemosensitivity in glioblastomas. Mol Cancer Ther 2005;4:1293–302.
28. Antonyak MA, Miller AM, Jansen JM, et al. Augmentation of tissue transglutaminase expression and activation by epidermal growth factor inhibit doxorubicin-induced apoptosis in human breast cancer cells. J Biol Chem 2004;279:41461–7.
29. Lorand L, Graham RM. Transglutaminases: crosslinking enzymes with pleiotropic functions. Nat Rev Mol Cell Biol 2003;4:140–56.
30. Mann AP, Verma A, Sethi G, et al. Overexpression of tissue transglutaminase leads to constitutive activation of nuclear factor-κB in cancer cells: delineation of a novel pathway. Cancer Res 2006;66:8788–95.
31. Akimov SS, Belkin AM. Cell-surface transglutaminase promotes fibronectin assembly via interaction with the gelatin-binding domain of fibronectin: a role in TGFβ-dependent matrix deposition. J Cell Sci 2001;114:2989–3000.
32. Hang J, Zemskov EA, Lorand L, Belkin AM. Identification of a novel recognition sequence for fibronectin within the NH_2-terminal β-sandwich domain of tissue transglutaminase. J Biol Chem 2005; 280:23675–83.
33. Akimov SS, Krylov D, Fleischman LF, Belkin AM. Tissue transglutaminase is an integrin-binding adhesion coreceptor for fibronectin. J Cell Biol 2000;148:825–38.
34. Strobel T, Cannistra SA. β_1-integrins partly mediate binding of ovarian cancer cells to peritoneal mesothelium *in vitro*. Gynecol Oncol 1999;73:362–7.
35. Cannistra SA, Ottensmeier C, Niloff J, Orta B, DiCarlo J. Expression and function of β_1 and $\alpha_v\beta_3$ integrins in ovarian cancer. Gynecol Oncol 1995;58:216–25.
36. Duxbury MS, Ito H, Benoit E, Waseem T, Ashley SW, Whang EE. RNA interference demonstrates a novel role for integrin-linked kinase as a determinant of pancreatic adenocarcinoma cell gemcitabine chemoresistance. Clin Cancer Res 2005;11:3433–8.
37. Yau CY, Wheeler JJ, Sutton KL, Hedley DW. Inhibition of integrin-linked kinase by a selective small molecule inhibitor, QLT0254, inhibits the PI3K/PKB/mTOR, Stat3, and FKHR pathways and tumor growth, and enhances gemcitabine-induced apoptosis in human orthotopic primary pancreatic cancer xenografts. Cancer Res 2005; 65:1497–504.
38. Maubant S, Cruet-Hennequart S, Dutoit S, et al. Expression of α_V-associated integrin β subunits in epithelial ovarian cancer and its relation to prognosis in patients treated with platinum-based regimens. J Mol Histol 2005;36:119–29.
39. Chan BM, Matsuura N, Takada Y, Zetter BR, Hemler ME. *In vitro* and *in vivo* consequences of VLA-2 expression on rhabdomyosarcoma cells. Science 1991; 251:1600–2.
40. Felding-Habermann B, O'Toole TE, Smith JW, et al. Integrin activation controls metastasis in human breast cancer. Proc Natl Acad Sci U S A 2001;98:1853–8.
41. Sawada K, Radjabi AR, Shinomiya N, et al. c-Met overexpression is a prognostic factor in ovarian cancer and an effective target for inhibition of peritoneal dissemination and invasion. Cancer Res 2007;67:1670–9.
42. Reinmuth N, Liu W, Ahmad SA, et al. $\alpha_v\beta_3$ integrin antagonist S247 decreases colon cancer metastasis and angiogenesis and improves survival in mice. Cancer Res 2003;63:2079–87.
43. Khalili P, Arakelian A, Chen G, et al. A non-RGD-based integrin binding peptide (ATN-161) blocks breast cancer growth and metastasis *in vivo*. Mol Cancer Ther 2006;5:2271–80.
44. Eble JA, Haier J. Integrins in cancer treatment. Curr Cancer Drug Targets 2006;6:89–105.
45. Facchiano F, Facchiano A, Facchiano AM. The role of transglutaminase-2 and its substrates in human diseases. Front Biosci 2006;11:1758–73.
46. Shibata K, Kikkawa F, Nawa A, Suganuma N, Hamaguchi M. Fibronectin secretion from human peritoneal tissue induces M_r 92,000 type IV collagenase expression and invasion in ovarian cancer cell lines. Cancer Res 1997;57:5416–20.

Enhanced Peritoneal Ovarian Tumor Dissemination by Tissue Transglutaminase

Minati Satpathy, Liyun Cao, Roxana Pincheira, et al.

Cancer Res 2007;67:7194-7202.